# Viscous coalescence of droplets – a Lattice Boltzmann study

M. Gross and I. Steinbach
*Interdisciplinary Centre for Advanced Materials Simulation (ICAMS), Ruhr-Universität Bochum, Stiepeler Strasse 129, 44801 Bochum, Germany*

D. Raabe
*Max-Planck Institut für Eisenforschung, Max-Planck Str. 1, 40237 Düsseldorf, Germany*

F. Varnik*
*Interdisciplinary Centre for Advanced Materials Simulation (ICAMS), Ruhr-Universität Bochum, Stiepeler Strasse 129, 44801 Bochum, Germany and Max-Planck Institut für Eisenforschung, Max-Planck Str. 1, 40237 Düsseldorf, Germany*

The coalescence of two resting liquid droplets in a saturated vapor phase is investigated by Lattice Boltzmann simulations in two and three dimensions. We find that, in the viscous regime, the bridge radius obeys a $t^{1/2}$-scaling law in time with the characteristic time scale given by the viscous time. Our results differ significantly from the predictions of existing analytical theories of viscous coalescence as well as from experimental observations. While the underlying reason for these deviations is presently unknown, a simple scaling argument is given that describes our results well.

## I. INTRODUCTION

Coalescence of liquid droplets is important in many technological and natural phenomena, as, for example, coating and sintering processes [1], phase separation of emulsions [2], or the formation of rain drops in clouds [3]. Coalescence is initiated when two droplets come into contact and form a liquid bridge, which then starts to grow due to surface tension. This growth is typically either opposed by viscous dissipation or inertial forces, until finally the two droplets have merged to a single droplet.

Assuming that the initial growth of the liquid bridge just results from a competition between surface tension $\sigma$ and fluid viscosity $\eta$, the characteristic velocity scale is given by the capillary velocity, $u_c = \sigma/\eta$. Taking the relevant length scale to be the size $b$ of the liquid bridge connecting the two droplets (see Fig. 1), a Reynolds number can be defined as $\mathrm{Re} = \rho u_c b/\eta = \rho\sigma b/\eta^2$. Due to the presence of $b$, this number will always be small in the beginning of the process, regardless of the value of $\sigma$ and $\eta$. The domain $\mathrm{Re} \lesssim 1$ then defines the *viscous regime*, which can be described by the Stokes equations, in contrast to the *inertial regime*, $\mathrm{Re} \gtrsim 1$, where the Euler equations hold. We remark that, recently [4], it has been suggested that the actual Reynolds number for the problem is in fact three orders of magnitude smaller than the estimate given above, resulting in an underestimation of the crossover time from the viscous to the inertial regime.

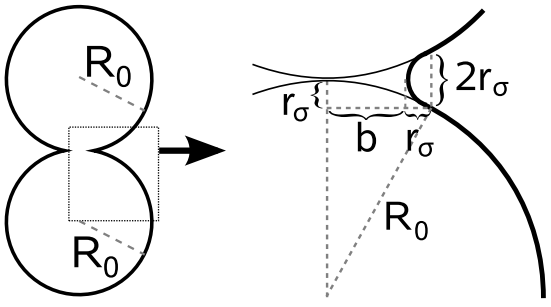


FIG. 1: Sketch of two coalescing droplets. $R_0$ is the droplet radius, $b$ the radius of the connecting bridge and $r_\sigma$ the radius of curvature of the meniscus. The right image is a magnification of the bridge region.

*Electronic address: fathollah.varnik@rub.de

Coalescence in the inertial regime is quite well understood nowadays [4–10] and it has been established theoretically and experimentally that the evolution of the bridge radius follows a scaling law of the form $b \propto (R_0\sigma/\rho)^{1/4}t^{1/2}$, where $R_0$ is the initial radius of each drop. However, for the viscous regime, there appear some discrepancies between experiments and theory up to today. The first effort to describe viscous coalescence dates back to the work of Frenkel [12] on viscous sintering of solid particles. By considering the balance between reduction of surface free energy and viscous dissipation, he derived a simple scaling law for the growth of the bridge radius, $b \propto (R_0\sigma/\eta)^{1/2}\, t^{1/2}$, which was confirmed in subsequent sintering experiments [13]. More sophisticated analysis of liquid droplet coalescence in the Stokes regime by Hopper [14] and Eggers et al. [15], aiming to overcome some of the simplifications of Frenkel's model, arrived at a characteristic $t^{0.86}$ or $t\log t$-growth law for the bridge radius at early times in the two- and three-dimensional case, respectively. However, subsequent experiments [4, 5, 7, 16] neither reproduced Frenkel's nor Eggers' results, but instead reported a linear time dependence, $b \propto \sigma t/\eta$ in the viscous regime [11]. The disagreement between theory and experiments was usually attributed to the asymptotic nature of the analytical results, which are expected to hold only in the limit of very small bridge radii. In a recent work, Paulsen et al. [17] resolve these discrepancies by arguing that most experiments have in fact not operated in the actual Stokes regime, but instead in a different, "inertially-limited" viscous regime where the drops are governed by a balance between surface tension, viscous forces and the center-of-mass inertia. In this new regime, droplets appear to follow a linear time evolution governed by the visco-capillary velocity $\sim \sigma/\eta$. In the following, however, it will usually not be essential to distinguish explicitly between the classical Stokes and the "inertially limited" viscous regime.

In this work, we study viscous coalescence of two droplets by Lattice Boltzmann computer simulations of a single-component fluid in two and three dimensions. We consider two quiescent droplets in a surrounding vapor phase for various values of surface tension, viscosity and vapor density. Interestingly, neither a growth of the bridge radius that is linear in time, as reported in experiments [4, 5, 7, 16], nor a growth as predicted by theories of Stokesian coalescence [14, 15] (i.e., $b \sim t^{0.86}$ in 2D or $b \sim -t\log t$ in 3D) is observed by us. Instead we find that the bridge radius is governed by an approximate $t^{1/2}$-scaling law, with the characteristic scale factor set by the viscous time – similar to Frenkel's original result. The underlying physical mechanism for our findings is presently unclear. Thus, despite the apparent simplicity of the problem, the present results suggest that the process of viscous coalescence is still not fully understood.

## II. SCALING THEORY

To aid the interpretation of our simulation results, we derive in this section a simple scaling law for coalescence that is based on the dominance of the viscous term in the Navier-Stokes equations. Note that, in the following, we employ a range of simplifications that occasionally deviate from assumptions made in the literature. However, our derivation is not intended as a correction of previous works, but instead is essentially motivated by its success in describing our simulation results. Fig. 1 shows the basic coalescence situation we consider in this work. $R_0$ is the initial radius of each of the two droplets, $b$ the radius of the connecting bridge, and $r_\sigma$ the radius of curvature of the meniscus. Due to rotational symmetry, it suffices to consider the problem in a plane that contains the conjoining line of the centers of the two droplets. By geometry, $R_0^2 = (b + r_\sigma)^2 + (R_0 - r_\sigma)^2$, and thus we obtain the radius of curvature as

$$r_\sigma = \frac{b^2}{2R_0} \cdot \frac{1}{1 - \frac{b}{R_0}} \approx \frac{b^2}{2R_0}\,, \tag{1}$$

where the last approximation is justified since we focus on $b \ll R_0$. It should be remarked that our estimate eq. (1) differs from a number of previous works [14, 15], which found $r_\sigma \sim b^3$. To obtain a relation for the time dependence of the bridge radius, we apply scaling arguments similar in spirit to [6, 15, 18] to the incompressible Navier-Stokes equations [19],

$$\rho(\partial_t + \mathbf{u}\cdot\nabla)\mathbf{u} = -\nabla p + \eta\nabla^2\mathbf{u}\,, \tag{2}$$

where $\rho$ is the density, $\mathbf{u}$ the fluid velocity and $p$ the local pressure. We shall neglect a possible rigid translation of the coalescing droplets (although, in principle, this effect can be relevant [14, 17]) and also ignore the influence of the vapor on the dynamics. Focusing now on the axis along the direction of the bridge radius, the flow velocity $u$ near the meniscus is, by continuity, determined by the motion of the bridge alone, $u = \dot{b}$. Assuming that the pressure varies between zero at the center of the bridge and the Laplace pressure $p_L \simeq -\sigma/r_\sigma$ at the curved meniscus, we can approximate $\nabla p \sim p_L/b$. Finally, we shall assume that the velocity varies smoothly (e.g., parabolically) between the center of the bridge (where $u \approx 0$) and the interface, allowing us to estimate $\nabla^2 u \sim -u/b^2$.

In the *viscous* regime, eq. 2 becomes $\eta\nabla^2 u = \nabla p_L$ and above simplifications lead to

$$\dot{b} = \frac{2R_0\sigma}{\eta}\frac{1}{b}\,. \tag{3}$$

The solution of this differential equation is easily written down as

$$b(t)^2 - b_0^2 = R_0^2\frac{t-t_0}{\tau}\,, \tag{4}$$

where $t_0$ is a suitably chosen initial time, $b_0 \equiv b(t_0)$ and the characteristic time scale $\tau$ is given by the viscous time

$$\tau_v = \eta R_0/4\sigma\,. \tag{5}$$

For completeness, we state also the result for the *inertial* regime, where the advection term $\rho(\mathbf{u}\cdot\nabla)\mathbf{u}$ dominates over the viscous stress. Here, the same solution as in eq. (4) is obtained, but with $\tau$ replaced by the inertial time

$$\tau_i = \sqrt{\rho R_0^3/8\sigma}\,. \tag{6}$$

It must be emphasized here that the above results hold independent of the spatial dimension.

Neglecting the integration constants $t_0$ and $b(t_0)$ in (4), which is justified for the intermediate and late stages of the evolution, the growth-law for the bridge radius can be expressed as

$$\boxed{\frac{b(t)}{R_0} \sim \left(\frac{t}{\tau_{v,i}}\right)^{1/2}\,.} \tag{7}$$

Of course, in the inertial regime, the above relation is already well known [6] and has been confirmed by experiments [4, 5, 7, 9, 16]. Remarkably, our simple scaling theory yields a power-law with the same exponent 1/2 also in the viscous regime, albeit with a different characteristic time scale. In sec. IV we present results of Lattice Boltzmann simulations that support eq. (7). Relation (7) agrees with Frenkel's classic result on viscous sintering [12], where it was obtained under the assumption that the two coalescing droplets reduce their surface free energy by moving closer together as a whole, without considering explicitly the dynamics of the bridge.

Clearly, it must be mentioned that our scaling result (7) differs from predictions of existing analytical theories of coalescence in the Stokesian regime in two and three dimensions, which predict a growth behavior like $b \sim t^{0.86}$ [14, 15] (see also sec. IV B). It also disagrees with most experiments on viscous coalescence that reported a linear time dependence, $b \sim t/\tau_v$ [4–7, 16]. (Note that, according to a recent proposition [17], these experiments have not been performed in the actual Stokes regime, but in the "inertially-limited" viscous regime, which apparently resolves the discrepancies between experiments and previous theories.) Of course, the scaling arguments leading to eq. (7) are not rigorous and therefore have to be taken with care. For instance, approximating the Laplacian of the velocity at the bridge as $\nabla^2 u \sim u/b^n$ with an arbitrary power $n$ allows one to write down a generalization of eq. (3) as

$$\dot{b} = \frac{2\sigma}{\eta}\left(\frac{b}{R_0}\right)^{n-3}\,.$$

Obviously, the choice $n = 2$ corresponds to eq. (7), supported by our simulations, while $n = 4$ would lead to a linear time dependence of $b$, in agreement with experiments. However, irrespective of the validity of the specific assumptions of our scaling theory, the fact that our simulations support eq. (7) indicates that the present understanding [17] of viscous coalescence is still incomplete and suggests that an unknown physical mechanism is possibly at work here.

## III. SIMULATION SETUP

Numerically, we solve the Navier-Stokes equation (2) in both two and three dimensions with the Lattice Boltzmann (LB) method, which is a well-established tool for fluid dynamical simulations ranging from the micro- to the macroscale [20]. Motivated by the growing interest in microfluidic applications, the LB method has been widely applied to the study of problems encompassing fluids in complex geometries or with multiple phases, such as droplet spreading or wetting [21]. For the study of coalescence, we employ an implementation of the LB model described in [8], which features faithful representation two-phase thermodynamics [22] as well as basic aspects of hydrodynamics [23]. The model is based on a Ginzburg-Landau description of a single-component fluid that allows for the coexistence of liquid

| | 2D | | | | | | | 3D | | | | | |
|---|---|---|---|---|---|---|---|---|---|---|---|---|---|
| Label | $\eta_L/\eta_V$ | $\sigma$ ($\times 10^{-4}$ l.u.) | $\tau_v$ ($\times 10^4$ l.u.) | $\tau_i$ | Oh l | Oh s | Re | $\eta_L/\eta_V$ | $\sigma$ ($10^{-4}$ l.u.) | $\tau_v$ ($\times 10^4$ l.u.) | $\tau_i$ | Oh | Re |
| ○ | 10 | 4.3 | 11 | 14 | 0.33 | 1.2 | 0.13 | 10 | 4.1 | 4.1 | 1.7 | 3.3 | 0.01 |
| △ | 1000 | 6.6 | 7.5 | 11 | 0.27 | 0.97 | 0.22 | 100 | 8.0 | 2.3 | 1.2 | 2.6 | 0.03 |
| □ | 100 | 1.3 | 3.9 | 8.0 | 0.20 | 0.70 | 0.40 | 1000 | 1.9 | 1.2 | 0.87 | 16 | 0.05 |
| ● | 10 | 3.3 | 20 | 16 | 0.52 | 1.8 | 0.05 | 10 | 3.3 | 5.6 | 2.0 | 4.0 | 0.006 |
| ▲ | 100 | 13 | 6.5 | 8.0 | 0.33 | 1.2 | 0.16 | 4 | 13 | 1.3 | 0.97 | 2.0 | 0.03 |

TABLE I: Parameters for our simulations in three and two dimensions. The first column refers to the symbols used in the plots, $\eta_L/\eta_V$ the liquid-vapor viscosity ratio (which is equal to the liquid-vapor density ratio), $\sigma$ the surface tension (in l.u.), $\tau_v$ and $\tau_i$ are the viscous and inertial times (in l.u.), Oh is the Ohnesorge number (see text) and Re is the average Reynolds number (the average is computed over the full coalescence process). In the 2D case, the letters 'l' and 's' below Oh refer to the simulations performed using a large ($R_0 = 5000$) or small ($R_0 = 400$) droplet radius. The values for $\tau_v$ and $\tau_i$ are stated for the smaller radius.

and vapor domains separated by a diffuse interface [24]. In the 2D case, two resting cylindrical droplets of identical radii of $R_0 = 5000$ lattice units (l.u.), initially separated by 4 l.u., are placed into a periodic rectangular domain of size $20100 \times 10200$ l.u. For comparison, we also performed simulations using droplet radii of $R_0 = 400$ and box sizes of $1800 \times 1000$ l.u. Due to computational limitations, the 3D simulations are performed with smaller system sizes of $460 \times 250 \times 250$, using two spherical droplets each of radius $R_0 = 100$ l.u., initially separated by 4 l.u. The initial separation of the two droplets has been varied in a few cases, showing that this parameter has a negligible influence on our results. Also, in a number of cases, simulations with larger system sizes have been performed to ensure that hydrodynamic interactions between periodic images are negligible. The bridge radius $b$ is determined from the (interpolated) position along the horizontal symmetry axis of the simulation box that corresponds to a density value of $(\rho_L + \rho_V)/2$. We follow the time evolution until the bridge radius has reached roughly half of the radius $R_0$ of the original droplets. We find that the volume of the liquid droplet stays constant during the whole coalescence process to a precision of $10^{-4}$. We have chosen comparable material parameters (i.e., viscosity, surface tension and density contrast between inner and outer fluid) to the silicon oil used in [5], amounting to typical droplet radii of a few mm and time units between 0.1 and 2 $\mu$s per l.u.. The viscous and inertial time scales range between 20 and 100 ms. Detailed simulation parameters can be found in Table I. We cover a wide range of values for surface tension, viscosity ratio (which is equal to the density ratio here), Ohnesorge and Reynolds number. The Ohnesorg number is defined as $\mathrm{Oh} = \eta/\sqrt{\rho_L \sigma R_0}$ and has been recently argued to be an important quantity separating different coalescence regimes [17]. According to the phase-diagram proposed in [17], the present values of the Ohnesorg number indicate that our simulations are located in the inertially-limited viscous regime. We will return to this point in sec. V.

As our LB simulations are based on a diffuse interface model [8, 24], some care is needed in order to avoid spurious influences of the finite interface width on the determination of the bridge radius. Denoting by $\xi$ the characteristic length scale over which the liquid-vapor interface is diffuse in our simulations, we have to make sure that we only consider the regime where all our physically interesting quantities are significantly larger than $\xi$, thereby approximating the sharp interface limit. This leads to the restrictions $b/\xi \gg 1$ for the bridge radius and $r_\sigma/\xi \gtrsim 1$ for the radius of curvature. While the first condition is easily fulfilled in our simulations, the latter one imposes a lower limit on the physically meaningful bridge radius. Using eq. (1) for the radius of curvature, $r_\sigma = b^2/2R_0$, one arrives at the condition

$$b/R_0 \gtrsim \sqrt{2\xi/R_0}\,. \tag{8}$$

With a typical value of $\xi = 4$, we obtain $b/R_0 \gtrsim 0.04$ for $R_0 = 5000$, $b/R_0 \gtrsim 0.15$ for $R_0 = 400$ and $b/R_0 \gtrsim 0.3$ for $R_0 = 100$.

## IV. RESULTS

### A. Two dimensions

In Fig. 2a, a typical coalescence event as obtained from our simulations is visualized (the behavior is similar in 3D). The upper inset of Fig. 2a shows the evolution of the center-of-mass position $\Delta y_{\mathrm{cms}} \equiv y_{\mathrm{cms}}(t) - y_{\mathrm{cms}}(0)$ of one of the droplets in dependence of the bridge radius $b/R_0$. For all our simulations, we find that the data is well described (including the proportionality constant) by a power-law $\Delta y_{\mathrm{cms}}/R_0 \simeq 0.3(b/R_0)^{3.4}$, represented by the solid line in the

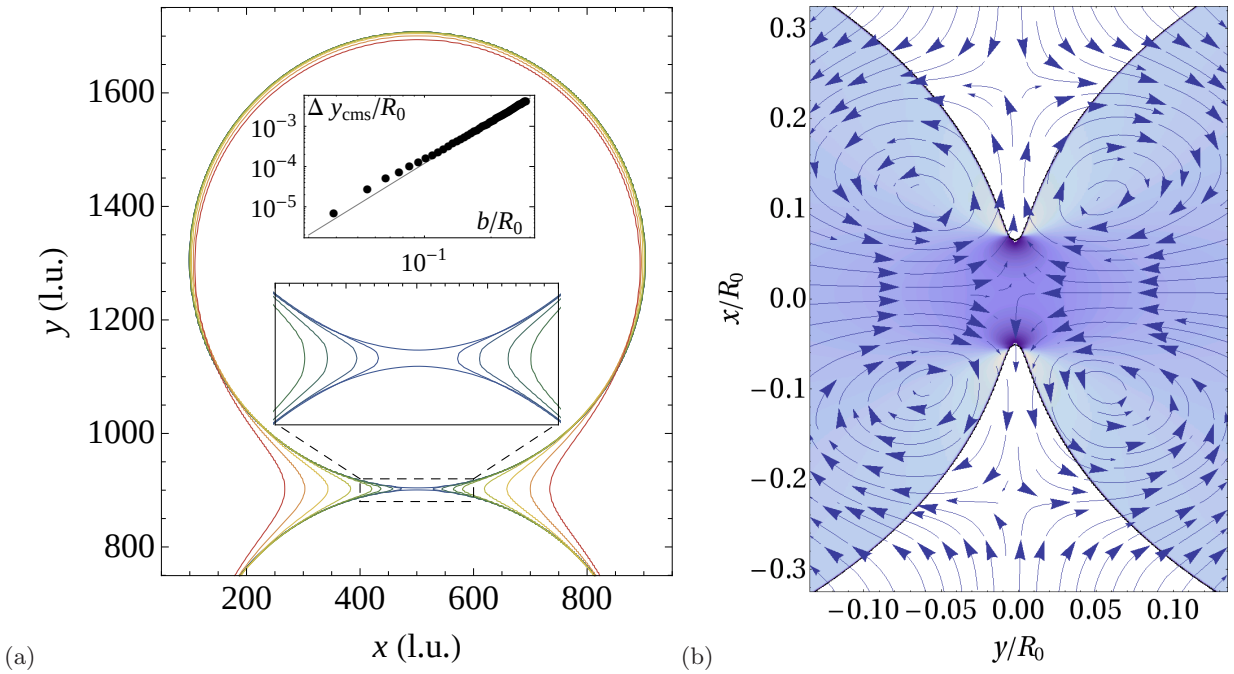


FIG. 2: (a) Coalescence of two droplets initially at rest (in 2D). Contours represent the interface liquid-vapor interface and correspond to times 0, 0.04, 0.1, 0.2, 0.3, 0.6, 1.0, 1.5, 2.0 (in units of $\tau_v$, from inner to outer). The bottom inset is a magnification of the bridge region. The upper inset shows the center-of-mass position, $\Delta y_{\rm cms} \equiv y_{\rm cms}(t) - y_{\rm cms}(0)$ of one of the droplets (measured along the symmetry axis) in a double-logarithmic representation. The solid line represents the prediction of Hopper [14]. (b) Velocity field at $t \simeq 0.3\tau_v$ close to the bridge. The color-field shows the pressure distribution (a darker color represents a larger pressure).

inset of Fig. 2a. Note that if one chooses to plot the data vs. $t/\tau_v$ rather than vs. $b/R_0$, a general power-law exponent of 1.7 is found, effectively in agreement with the predictions of the Stokesian theory coalescence by Hopper [14]. In this representation, the prefactor, however, turns out to be strongly dependent on the droplet size. The exponent 3.4 that describes the dependence of $\Delta y_{\rm cms}$ on $b/R_0$ can be obtained from Hopper's theory by substituting the proper time-dependence of the bridge radius as observed in the present simulations ($b \sim t^{0.5}$, see below).

Fig. 2b shows the velocity field close to the bridge, together with the pressure distribution inside the droplet. As expected, the pressure is largest at the meniscus. Since we are simulating coexisting liquid and vapor phases separated by a diffuse interface, there occur no flow discontinuities. Note that in typical experiments, droplets are composed of a different material than the surrounding fluid phase (as characteristic for emulsions) [4–7, 16].

Fig. 3a presents the raw data of the time evolution of the bridge radius obtained from five simulations with different sets of simulation parameters (see Table I). From the values of the Reynolds number (see inset) it can already be inferred that the coalescence process is dominated by viscosity. This is also corroborated by the (approximate) data collapse obtained when rescaling the time axis with the viscous time $\tau_v$ [eq. (5)], as seen in Fig. 3b. In contrast, when expressing the time in units of the inertial time $\tau_i$, no collapse is obtained. As Fig. 3c shows, the bridge radius follows an approximate $t^{1/2}$-law over almost two decades in time, well agreeing with the predictions of our scaling analysis [eq. (7)]. The actual exponent is found to differ slightly between the individual curves, being in the range of $0.50 - 0.58$. These minor discrepancies should not be surprising given the strong simplifications used to arrive at eq. (7). Note that there are no fitting parameters involved in obtaining the plots.

For comparison, Fig. 4 shows data for bridge radius obtained for droplets of radius $R_0 = 400$, using the same set of simulation parameters as in Fig. 3. Due to the smaller droplet radii, the evolution spans only about one decade in time. Nevertheless, from the time rescaling (Fig. 4a) and logarithmic representation (Fig. 4b) we again conclude that the droplets coalesce in the viscosity-dominated regime, following a $t^{1/2}$-law in time.

The presence of a $t^{1/2}$-scaling law in the viscous regime is unexpected on the basis of previous experiments on coalescence of two-dimensional liquid lenses [7], which reported a linear time evolution for the bridge radius (similar to the 3D case). An analytical theory for Stokesian coalescence by Hopper [14] predicts that $b \propto (t/\tau_v)^{0.857}$ in the range $0.003 < b/R_0 < 0.15$ (at later times, the evolution $b$ gradually slows down until the coalescence process comes to an end). Note, however, that, according to the recent study of Paulsen et al [17] our simulations reside in the inertially-limited viscous regime, where the predictions of Stokesian theories are not valid. Coming back our simulation

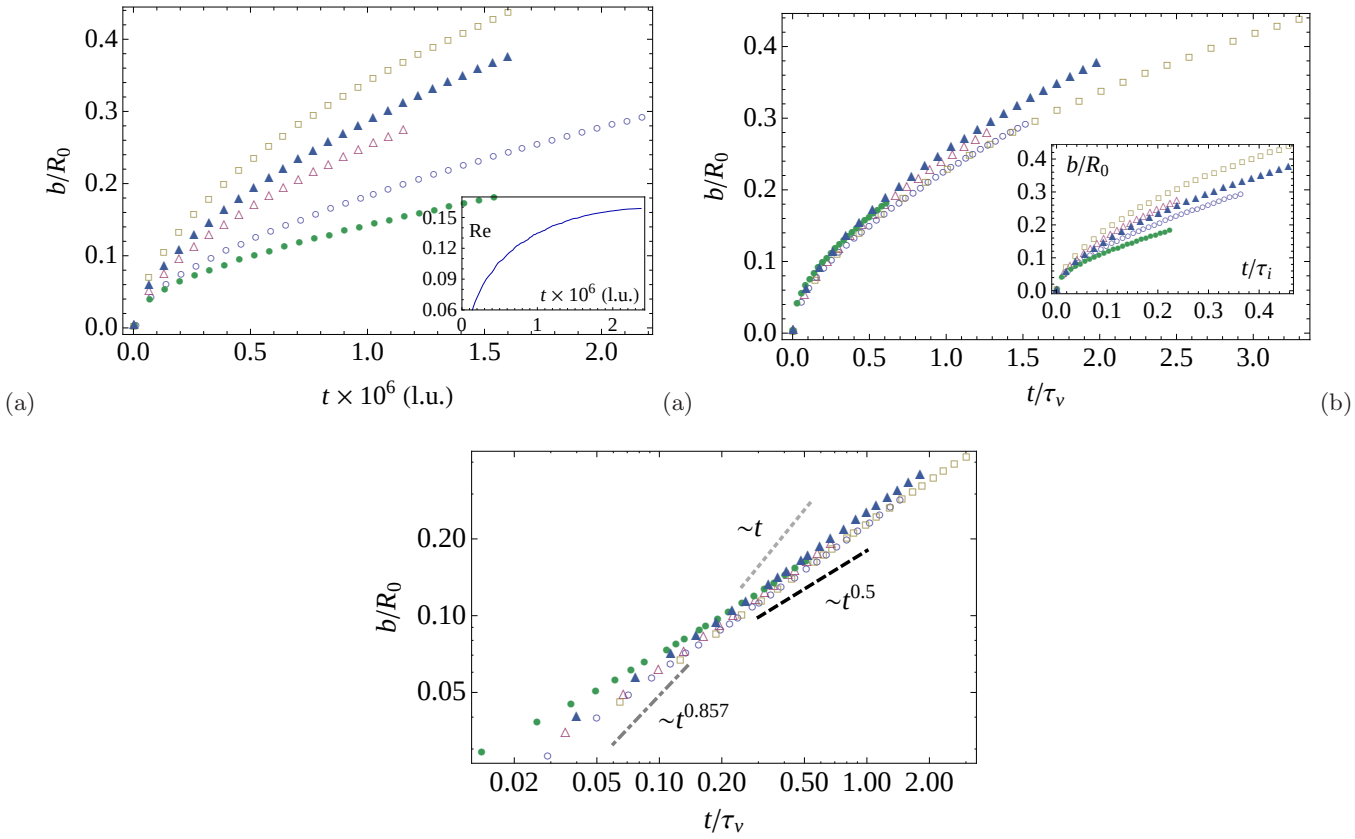


FIG. 3: Viscous coalescence in 2D for two droplets of initial radius $R_0 = 5000$ l.u. (a) Raw data for the time evolution of the bridge radius $b$ (in units of the droplet radius $R_0$) as obtained from our simulations. The inset shows the evolution of the Reynolds number for one case. In (b), the data is shown when the time is expressed in terms of the viscous time $\tau_v$. For comparison, in the inset, time is rescaled by the inertial time $\tau_i$. In (c), the data is plotted in a double-logarithmic representation using the same rescaling of the axes as in (b). The dashed, dot-dashed and dotted lines represent power laws $\sim t^{1/2}$, $\sim t^{0.857}$ and $\sim t$, respectively. See Table I for a legend to the different symbols.

results, it is clearly visible from Fig. 3b and c that there appears no sufficiently extended region where either a linear or $t^{0.857}$-law can describe the data well.

### B. Three dimensions

Turning to the three-dimensional problem, we proceed in an analogous manner as for the 2D case. In Fig. 5a we show the bridge radius evolution obtained from five representative simulation runs (see Tab. I for simulation parameters). Although simulation parameters are comparable to 2D, the Reynolds number remains roughly one order of magnitude smaller than in two dimensions. As seen in Fig. 5b, expressing the time in units of the viscous time, $\tau_v$, produces a reasonable scaling collapse of all data points onto a master curve. In contrast, no collapse is found when rescaling the time with the inertial time $\tau_i$ (inset to Fig. 5b). This confirms, independently from the value of the Reynolds number, the dominance of viscosity in the coalescence process. As the double-logarithmic representation of Fig. 5c shows, the data follows our predicted $t^{1/2}$-scaling law [eq. (7)] with reasonable accuracy. The power-law exponent is found to be only approximately equal to 1/2, but instead varying in the range $0.45 - 0.6$ between the individual curves. It is remarked that, due to computational limitations, the initial radii of the two droplets had to be chosen significantly smaller than in 2D and, consequently, the time axis in Fig. 5 spans only roughly one decade. This range is nevertheless comparable to experiments [5, 16]. Note also that no fitting parameters are involved in our representation of the data.

Similarly as in the two-dimensional case, even when acknowledging the slight variation in the power-law exponent, our results stand in remarkable contrast to experiments [4, 5, 16], where typically a linear time-dependence is observed (see, however, [11]). It is also interesting to compare our results to the analytical theory of three-dimensional

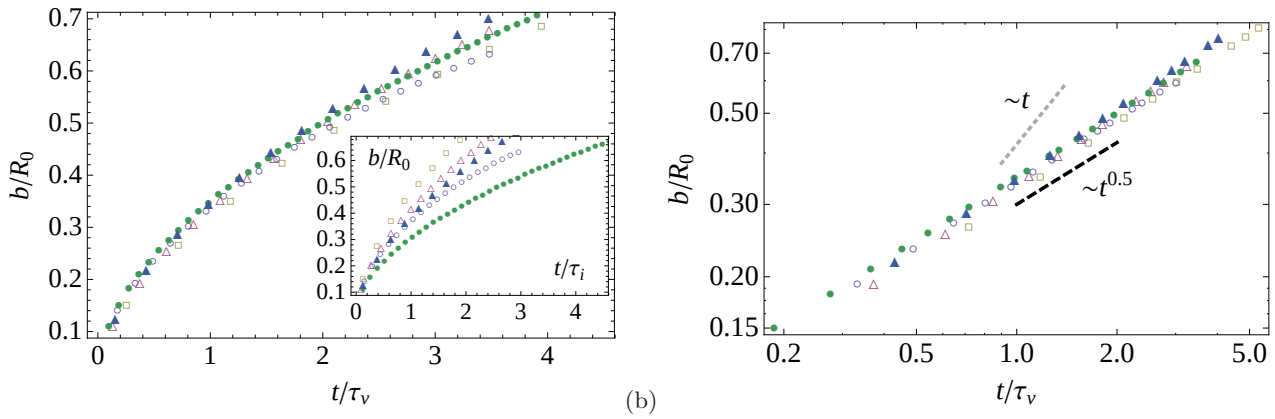


FIG. 4: Viscous coalescence in two dimensions for two droplets of initial radius $R_0 = 400$ l.u. Time is expressed in terms of the viscous time $\tau_v$, while the bridge radius $b$ is expressed in units of $R_0$. For comparison, in the inset, the time is rescaled by the inertial time $\tau_i$. In (a), the data is shown in a linear and in (b) in a double-logarithmic representation. The dashed and dotted lines represent power laws $\sim t^{1/2}$ and $\sim t$, respectively. See Table I for a legend to the different symbols.

coalescence of Eggers et al. [15], which predicts the bridge radius (in the region $r_b \lesssim b \lesssim R_0$) to evolve according to the differential equation

$$\frac{\dot{b}(t/\tau_v)}{R_0} = -\frac{1}{2\pi} \log\left( c_0 \left[ \frac{b(t/\tau_v)}{R_0} \right]^{\alpha-1} \right) , \tag{9}$$

where $c_0$ and $\alpha$ are constants that, in the original work [15], are predicted as $c_0 = 1$ and $\alpha = 3$ for an inviscid outer fluid while $\alpha = 3/2$ for finite viscosity ratios (both valid for $b/R_0 \ll 1$). For $b \lesssim 0.03 R_0$, the solution of eq. (9) follows an approximate scaling law of the form [15]

$$\frac{b\,(t/\tau_v)}{R_0} \sim \frac{t}{\tau_v} \log\left( \frac{t}{\tau_v} \right) . \tag{10}$$

In Fig. 6a, the typical behavior of the numerical solution of eq. (9) as well as the approximate law (10) is shown. Several interesting observations can be made: First of all, at any time the bridge radius as predicted by the analytical theory evolves significantly slower than it would be for a linear time-dependence. In fact, over many decades, the early-time behavior of eqs. (9) and (10) can be fitted by an effective power-law $\sim t^{0.86}$, whose exponent is practically identical to the value obtained by Hopper in the two-dimensional case [14]. At longer times, the evolution of the bridge slows down and a time window appears where $b$ approximately evolves as $t^{0.5}$.

Given this observation, it is tempting to fit the numerical solution of eq. (9) to our data for the bridge radii (Fig. 6b). We find that reasonable agreement can only be obtained if $\alpha$ and $c_0$ are treated as fit parameters. In the inset to Fig. 6b it is seen that the obtained best-fit values for the scaling exponent $\alpha$ decrease with the liquid-vapor viscosity ratio $\eta_L/\eta_V$, settling around a value of 2 for large viscosity ratios – a trend which is opposite to the theoretical predictions of [15]. The parameter $c_0$ is found to be of the order of unity for all except the smallest viscosity ratios – a result which roughly agrees with the theoretical expectation, $c_0 = 1$. Due to the limited range in time, it can presently not be decided whether our observation of a $t^{1/2}$-law in the data for three-dimensional coalescence (Fig. 5c) is a manifestation of a finite-size effect associated with the slowing-down of the coalescence process or whether it actually represents a true deviation from the Stokesian theory of coalescence [15], similar to the two-dimensional case. Here, additional simulations over a much larger range of time will be necessary to clarify this issue. This is reserved for future work.

## V. SUMMARY

In this work, we have investigated the coalescence of two identical resting droplets in the viscous regime in two and three dimensions. ¿From Lattice Boltzmann simulations of the full isothermal Navier-Stokes equations for a non-ideal fluid, we find that the time evolution of the bridge radius can be well described by a $t^{1/2}$-scaling law – in striking similarity to what is well-known to hold in the inertial regime, albeit with a different characteristic time constant. We

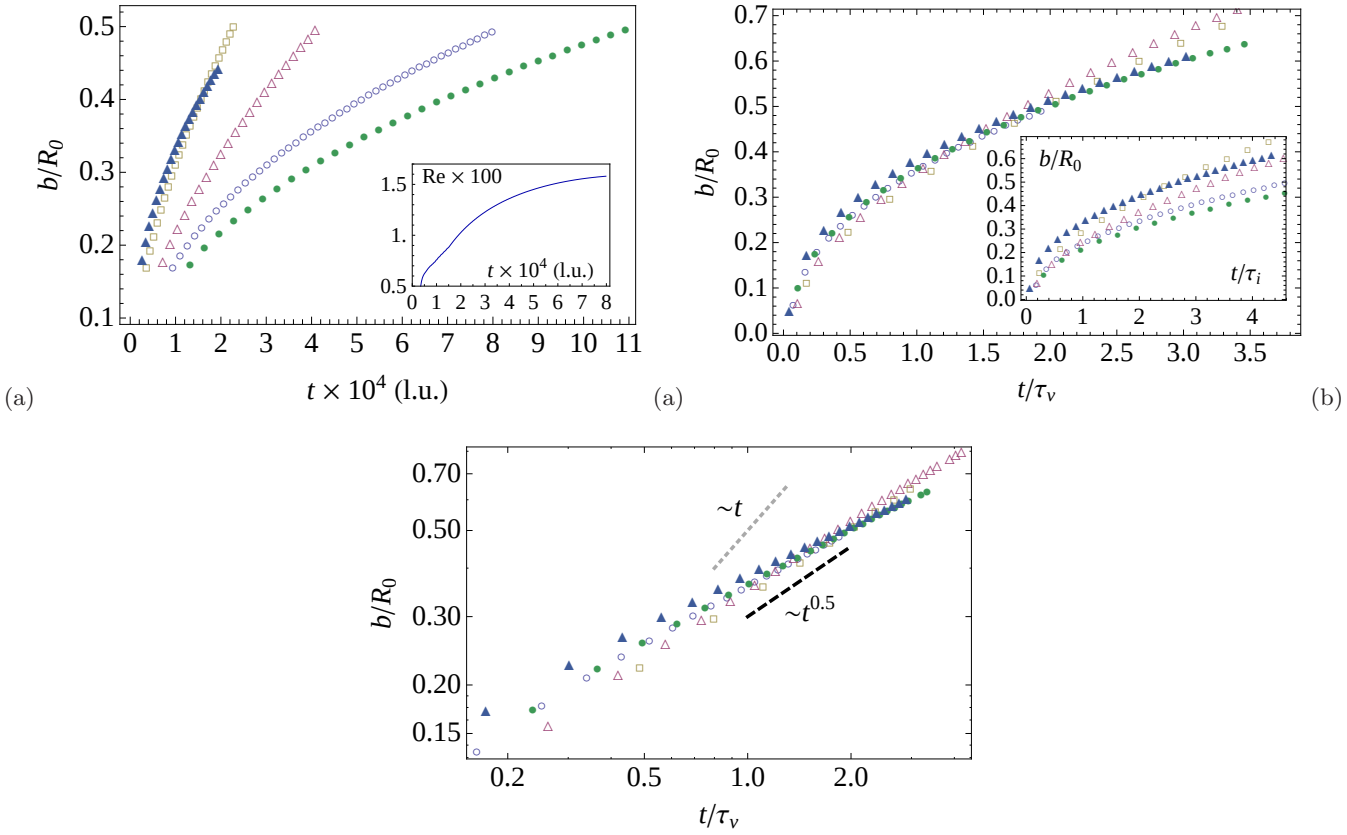


FIG. 5: Viscous coalescence in 3D. (a) Raw data for the time evolution of the bridge radius $b$ (in units of the droplet radius $R_0$) as obtained from our simulations. The inset shows the evolution of the Reynolds number for one case. In (b), the data is shown when the time is expressed in terms of the viscous time $\tau_v$. For comparison, in the inset, time is rescaled by the inertial time $\tau_i$. In (c), the data is plotted in a double-logarithmic representation using the same scaling of the axes as in (b). The dashed and dotted lines represent power laws $\sim t^{1/2}$ and $\sim t$, respectively. See Table I for a legend to the different symbols.

have shown that our simulation results can be rationalized through simple scaling arguments applied to the Stokes equations [see eq. (4)]. Although similar material parameters are used (leading, for instance, to similar values of the Ohnesorg-number [17]), our results differ significantly from recent experiments [4, 5, 7, 7, 16], which report a linear time-evolution of the bridge radius in the viscous regime both in two and three dimensions. In two dimensions, our findings for the evolution of the bridge radius are also clearly different from analytical theories [14], which predict a power-law $b \sim t^{0.86}$. The center-of-mass motion of each droplet is found to be described by a power-law $\sim t^{1.7}$, with an exponent that, surprisingly, agrees well with the theoretical prediction [14]. Due to the limited range in time, no definite conclusions concerning possible agreement with the theory for three-dimensional Stokesian coalescence [15] can be drawn presently. It is useful to remark that, in the language of the phase-diagram of [17], our simulations are located in the inertially-limited viscous regime – the region where in fact also most experiments [4, 5, 7, 7, 16] reside. In the light of this, it is not surprising that our simulations disagree with the theoretical predictions obtained in the Stokes regime, which applies to droplets of much larger viscosity than presently used. It should be noted that the time-evolution of the bridge radius in the inertially-limited viscous regime is only empirically characterized by a linear law. A theoretical derivation of this scaling law appears to be lacking so far.

Presently, an explanation for the discrepancies between our work and existing theories or experiments remains elusive. We remark, however, that, in contrast to experiments, we study here the dynamics of a liquid droplet surrounded by its own vapor. Although we find that the total volume of the droplet is conserved to $O(10^{-4})$, significant local evaporation and condensation processes can be present in regions of large curvature. These, in turn, might change the dynamics of the bridge and be ultimately responsible for the observed $t^{1/2}$ scaling law. Also, in contrast to predictions of [15], we have never observed the presence of a vapor bubble around the neck. These issues should be considered in future investigations.

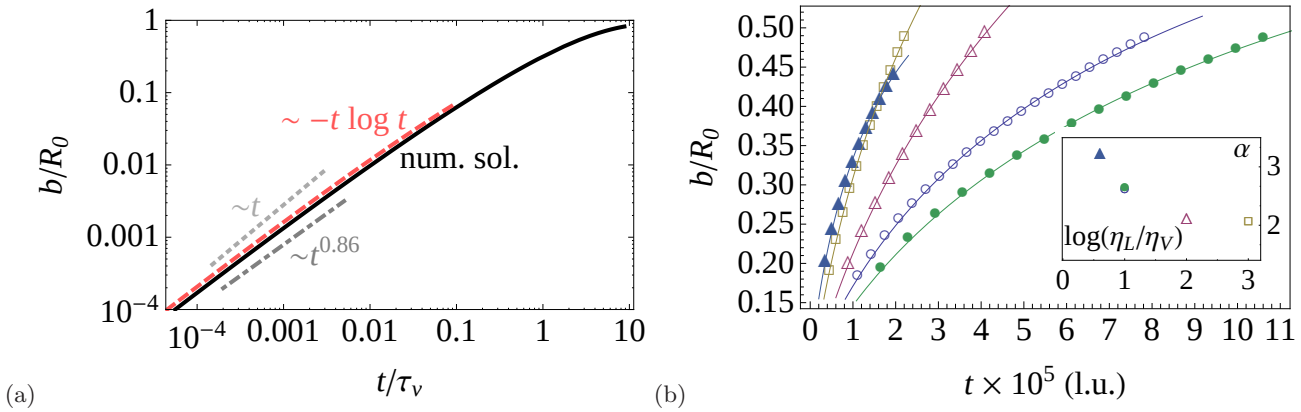


FIG. 6: (a) Theoretical time evolution of the bridge radius according to the numerical solution of eq. (9) (•) and its asymptotic approximation [eq. (10), dashed], for a typical set of droplet parameters. At early times, the analytical predictions can be well approximated by an effective power-law $b \sim t^{0.86}$. For comparison, also a linear power-law ($b \sim t$) is indicated. (b) Numerical solution of eq. (9) (solid curves) fitted to the data for the bridge radius $b$ obtained from simulations in 3D (symbols). The inset shows the dependence of the fit parameter $\alpha$ on the liquid-vapor viscosity ratio. Error bars are of the order of the symbol size.


### Acknowledgments

We thank K. Stratford and D. Bonn for useful discussions and an anonymous referee for valuable suggestions. Financial support by the Deutsche Forschungsgemeinschaft (DFG) under the grant number Va205/3-3 (within the Priority Program SPP1164) is acknowledged. ICAMS acknowledges funding from its industrial sponsors, the state of North-Rhine Westphalia and the European Commission in the framework of the European Regional Development Fund (ERDF).



[1] C. J. Brinker and G. W. Scherrer, *Sol-Gel Science* (Academic Press, 1990).

[2] V. S. Nikolayev, D. Beysens and P. Guenoun, "New hydrodynamic mechanism for drop coarsening," Phys. Rev. Lett. **76**, 3144 (1996).

[3] Z. Hu and R. C. Srivastava, "Evolution of raindrop size distribution by coalescence, breakup, and evaporation: Theory and observations," J. Atmos. Sci. **52**, 1761 (1995).

[4] J. D. Paulsen, J. C. Burton and S. R. Nagel, "Viscous to inertial crossover in liquid drop coalescence," Phys. Rev. Lett. **106** 114501, (2011).

[5] D. G. A. L. Aarts, H. N. W. Lekkerkerker, H. Guo, G. H. Wegdam and D. Bonn, "Hydrodynamics of droplet coalescence," Phys. Rev. Lett. **95** 164503, (2005).

[6] L. Duchemin, J. Eggers and C. Josserand, "Inviscid coalescence of drops," J. Fluid Mech. **487**, 167 (2003).

[7] J. C. Burton and P. Taborek, "Role of dimensionality and axisymmetry in fluid pinch-off and coalescence," Phys. Rev. Lett. **98**, 224502 (2007).

[8] T. Lee and P. F. Fischer, "Eliminating parasitic currents in the lattice Boltzmann equation method for nonideal gases," Phys. Rev. E **74**, 046709 (2006).

[9] A. Menchaca-Rocha, A. Martinez-Davalos, R. Nunez, S. Popinet and S. Zaleski, "Coalescence of liquid drops by surface tension," Phys. Rev. E **63**, 046309 (2001); M. Wu, T. Cubaud and C.-M. Ho, "Scaling law in liquid drop coalescence driven by surface tension," Phys. Fluids **16**, L51 (2004); S. C. Case and S. R. Nagel, "Coalescence in low-viscosity liquids," Phys. Rev. Lett. **100**, 084503 (2008).

[10] S. T. Thoroddsen, K. Takehara and T. G. Etoh, "The coalescence speed of a pendent and a sessile drop," J. Fluid Mech. **527**, 85 (2005).

[11] An exception to this is the experiment of [10], where, in a one case, an $t^{1/2}$-behavior was observed for $b \gtrsim 0.2R_0$.

[12] J. Frenkel, "Viscous flow of crystalline bodies under the action of surface tension," J. Phys. (Moscow) **9**, 385 (1949).

[13] G. C. Kuczynski, "Study of the sintering of glass," J. Appl. Phys. **20**, 1160 (1949); W. D. Kingery and M. Berg, "Study of the initial stages of sintering solids by viscous flow, evaporation-condensation, and self-diffusion," J. Appl. Phys. **26**, 1205 (1955).

[14] R. W. Hopper, "Coalescence of Two Equal Cylinders: Exact Results for Creeping Viscous Plane Flow Driven by Capillarity" J. Am. Ceram. Soc. **67**, C262 (1984).

[15] J. Eggers, J. R. Lister and H. A. Stone, "Coalescence of liquid drops," J. Fluid Mech. **401**, 293 (1999).

[16] W. Yao, H. J. Maris, P. Pennington and G. M. Seidel, "Coalescence of viscous liquid drops," Phys. Rev. E **71**, 016309 (2005). Here, an exponential scaling function with an almost linear regime at small times was found.
[17] J. D. Paulsen, J. C. Burton, S. R. Nagel, S. Appathurai, M. T. Harris and O. A. Basaran, "The inexorable resistance of inertia determines the initial regime of drop coalescence", Proc. Nat. Acad. Sci. **109**, 6857 (2012).
[18] R. D. Narhe, D. A. Beysens and Y. Pomeau, "Dynamic drying in the early-stage coalescence of droplets sitting on a plate," EPL **81**, 46002 (2008).
[19] L. D. Landau and E. M. Lifshitz, *Fluid Mechanics* (Pergamon, New York, 1959).
[20] S. Succi, *The Lattice Boltzmann Equation for Fluid Dynamics and Beyond* (OUP, Oxford, 2001); C. K. Aidun and J. F. Clausen, "Lattice-Boltzmann method for complex flows," Annu. Rev. Fluid Mech. **42** 439 (2010);
[21] P. Raiskinmäki, A. Koponen, J. Merikoski and J. Timonen, "Spreading dynamics of three-dimensional droplets by the lattice-Boltzmann method," Comput. Mater. Sci. **18**, 7 (2000); A. Dupuis and J. M. Yeomans, "Modeling droplets on superhydrophobic surfaces: equilibrium states and transitions," Langmuir **21**, 2624 (2005); F. Varnik, P. Truman, B. Wu, P. Uhlmann, D. Raabe and M. Stamm, "Wetting gradient induced separation of emulsions: A combined experimental and lattice Boltzmann computer simulation study," Phys. Fluids **20**, 072104 (2008); N. Moradi, F. Varnik and I. Steinbach, "Contact angle dependence of the velocity of sliding cylindrical drop on flat substrates", EPL **95**, 4403 (2011).
[22] E. S. Kikkinides, A. G. Yiotis, M. E. Kainourgiakis and A. K. Stubos, "Thermodynamic consistency of liquid-gas lattice Boltzmann methods: Interfacial property issues," Phys. Rev. E **78**, 036702 (2008).
[23] M. Gross, N. Moradi, G. Zikos and F. Varnik, "Shear stress in nonideal fluid lattice Boltzmann simulations", Phys. Rev. E **83**, 017701 (2011).
[24] D. M. Anderson, G. B. McFadden and A. A. Wheeler, "Diffuse-interface methods in fluids mechanics," Annu. Rev. Fluid. Mech. **30**, 139 (1998).